ELSEVIER

Contents lists available at ScienceDirect

#### Sustainable Cities and Society

journal homepage: www.elsevier.com/locate/scs



# Propagating epistemic uncertainties in planning and design of energy efficient districts

Mohsen Sharifi <sup>a,c,\*</sup>, Amin Kouti <sup>a,c</sup>, Mohammad Haris Shamsi <sup>d</sup>, Rui Guo <sup>b</sup>, Dirk Saelens <sup>b,c</sup>

- a VITO. Water and energy transition unit, Mol. Belgium
- <sup>b</sup> KU Leuven, Leuven, Belgium
- c EnergyVille, Genk, Belgium
- d Energy Institute, The Bartlett School of Architecture, University College London, London, UK

#### ARTICLE INFO

# Keywords: Data-driven energy modeling Epistemic uncertainty Dempster-shafer theory Energy Efficient Districts Urban Building Energy Modeling

#### ABSTRACT

Urban energy planning and design are inherently challenged by a lack of granular input data, resulting in epistemic uncertainties. This study focuses on methodologies to quantify and propagate these uncertainties to support decision-making in urban energy planning. Specifically, we examine the use of clustering techniques, commonly applied to model districts with limited building archetypes. We demonstrate and measure uncertainties that archetype modeling introduces in the outcomes. To this aim, we developed a novel methodology grounded in Dempster-Shafer theory (DST) of evidence and demonstrate it using a case study district in Belgium. Using the EnergyVille Building Energy Calculation System (EBECS) and a metaheuristic optimization algorithm. we evaluate two collective decarbonization scenarios targeting 60 % and 80 % reductions in operational carbon emissions for residential buildings across the district. We propose methods to derive sub-archetypes, and their probability mass functions within each archetype. Then, belief and plausibility functions are calculated to predict distribution functions of outcomes, while saving a significant number of required simulations in comparison to existing methods such as Monte Carlo simulations that are prohibitive at an urban scale. Our results reveal that the 60 % reduction scenario, while appearing cost-effective under deterministic assumptions, carries high uncertainty, potentially leading to higher carbon abatement costs than predicted. In contrast, the 80 % scenario is more robust under low-uncertainty conditions. This research demonstrates the critical role of uncertainty quantification as a key performance indicator in urban energy planning, supporting decision-makers in mitigating financial and environmental risks.

#### 1. Introduction

Urban energy demand continues to rise and will increase substantially due to rapid urbanization, with over two-thirds of the global population expected to reside in urban areas by 2050 (IEA, 2024). Cities need to become more energy-efficient, sustainable, and resilient to climate change to cope with this rapid urbanization. This often involves retrofitting existing buildings (BPIE - Buildings Performance Institute Europe, 2021), (IEA, 2022) to enhance energy performance, integrating local renewable energy sources to maximize self-sufficiency, and

reducing operational carbon emissions (Esfandi et al., 2024;IEA, 2024; IEA, 2021). Finding solutions to reduce carbon emissions while also minimizing expenses is a complex, multidimensional process (Araújo, Gomes, Ferrão & Gomes, Dec., 2024). Planning without considering uncertainties can lead to over- or under-investment, potentially jeopardizing the cost-effectiveness of proposed strategies. Moreover, uncertainty quantification ensures that resources are allocated to measures with the highest likelihood of achieving desired outcomes to support successful policymaking (Asadi, Chenari, Gaspar & Gameiro da Silva, May, 2023). In this process, urban building energy modeling (UBEM) is a

List of Abbreviations: BPAs, Basic Probability Assignments; CBF, Cumulative Belief Function; CDF, Cumulative Distribution Function; CPF, Cumulative Plausibility Function; DEAP, Distributed Evolutionary Algorithms in Python; DST, Dempster–Shafer Theory (of Evidence); EBECS, EnergyVille Building Energy Calculation System; EPC, Energy Performance Certificate; GDPR, General Data Protection Regulation; HVAC, Heating, Ventilation, and Air Conditioning; KPI, Key Performance Indicator; MCS, Monte Carlo Simulation; PDF, Probability Density Function; RMSSTD, Root Mean Square Standard Deviation; SA, Sensitivity Analysis; TCO, Total Cost of Ownership; UA, Uncertainty Analysis; UBEM, Urban Building Energy Modeling; WWR, Window-to-Wall Ratio.

E-mail address: mohsen.sharifi@vito.be (M. Sharifi).

https://doi.org/10.1016/j.scs.2025.106520

Received 3 March 2025; Received in revised form 3 June 2025; Accepted 4 June 2025 Available online 9 June 2025

2210-6707/© 2025 The Authors. Published by Elsevier Ltd. This is an open access article under the CC BY-NC license (http://creativecommons.org/licenses/by-nc/4.0/).

<sup>\*</sup> Corresponding author.

tool that supports urban planners for informed decision-making and optimal urban energy planning. UBEM outcomes are subject to two distinct types of uncertainties: epistemic and aleatoric. Epistemic uncertainties arise from incomplete knowledge, input data limitations, or model simplifications, which are reducible with more information. Aleatoric uncertainties, on the other hand, stem from inherent randomness and variability in weather conditions, energy prices, and occupant behavior, making them irreducible. Fig. 1 illustrates the relation between total uncertainties and its epistemic and aleatoric nature. Epistemic uncertainties can be decreased to a certain level by more data gathering. Aleatoric uncertainties can be only reported to help decision-makers to search for risk mitigation options. This paper focuses on developing a method to quantify epistemic uncertainties resulting from simplifications and lack of quality data that are inevitable in large-scale analyses in urban building energy modeling and simulations. The application of the proposed method is demonstrated for residential building stock in a Belgian district due to the availability of detailed EPC data, relevance to policy frameworks.

The paper is structured as follows. Section 1 reviews the existing literature on UBEM, highlighting current methodologies, key limitations, sources of uncertainties, and methods for uncertainty quantification and the need for this study. Section 2 elaborates on the methodology used in this study, including data collection, clustering buildings to derive archetypes, building retrofit strategy development, and the developed uncertainty propagation method based on Dempster-Shafer theory (DST) of evidence. Section 3 provides information about the case study used in the article. Section 4 presents the results of the case study, discussing how input data quality, retrofit strategies, and investment cost uncertainties can influence expected operational carbon emissions from buildings and cost-effectiveness of building retrofits. Section 5 presents discussions about implications of the findings, limitations of this study, and recommendations for future research. Finally, Section 6 provides conclusions, emphasizing the need for scalable and flexible UBEM models that incorporate uncertainty quantification to guide policy- and decision-making.

#### 1.1. Urban building energy modelling: existing tools and practices

UBEM serves as a critical tool for managing the complexity of

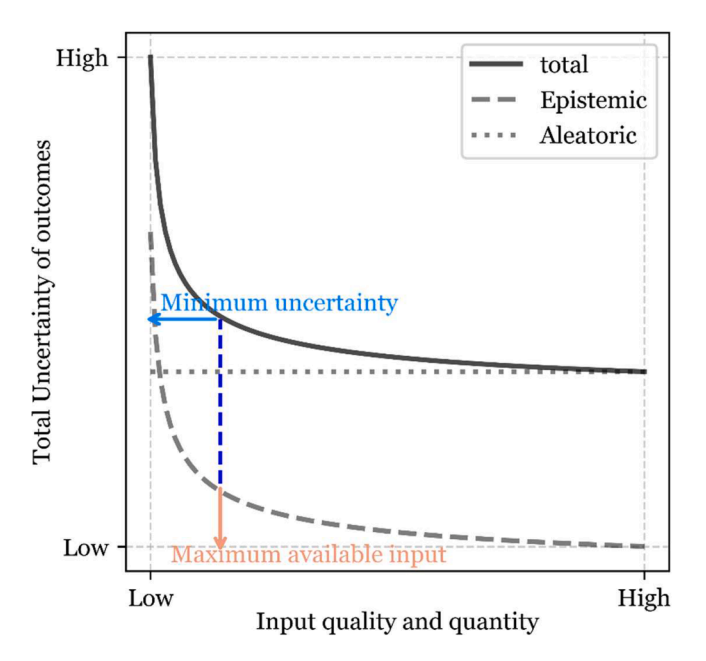


**Fig. 1.** Conceptual relation between total uncertainty with epistemic and aleatoric uncertainties. Blue dashed line shows minimum epistemic uncertainty that must be quantified.

modern urban energy systems, particularly in the pursuit of sustainable, resilient, and energy-efficient cities (Deng, Javanroodi, Nik & Chen, Sep., 2023). By simulating the energy performance of buildings at the city or district scale, UBEM empowers planners to evaluate the intricate trade-offs between energy efficiency, costs, carbon emissions, and social equity. UBEM facilitates informed decision-making on retrofitting measures, renewable energy generation strategies, and policy interventions, all while considering economic and social implications.

UBEM methodologies generally adopt either bottom-up or top-down modeling approaches. Top-down models treat the entire building sector as a single or very limited number of elements to estimate energy consumption on a large scale in national level. In contrast, bottom-up modeling approaches analyze individual buildings and their end-uses, estimating energy consumption at the level of single buildings or groups of buildings (Ali et al., Sep., 2021). Bottom-up modelling requires detailed physical attributes such as construction materials, geometry, and heating and cooling and air conditioning (HVAC) systems (Kamel, Nov., 2022). Conversely, top-down models leverage statistical or econometric methods to estimate energy consumption using aggregated data, including historical energy use, socio-economic factors, and urban density (Wong et al., Nov., 2021), more applicable on national level energy modeling.

Bottom-up models are developed using building energy simulation engines like EnergyPlus (EnergyPlusTM, 2017), accompanied by programs such as CityBES (Chen et, al.), and URBANopt (El Kontar et al., 2020) hosting integrated tools for post-processing and optimization tasks to derive optimal design on urban scale. Also, building models in the bottom-up approach can be developed with in-house developed tools tailored for available input data.

To further streamline complex urban models, similar buildings are grouped into representative archetypes, reducing computational demands while maintaining reasonable accuracy (Dahlström, Johari, Broström & Widén, Jan., 2024). These building archetypes are often derived using clustering techniques complemented with expert analysis for fine-tuning and sanity check (Guo, Bachmann, Kersten & Kriegel, 2023), (Prina et al., 2024). A common approach is to use Energy Performance Certificates (EPC) of buildings as the basis and use data analysis to provide essential inputs for energy simulations in UBEM. For instance, Johari et al. developed a UBEM using geo-referenced EPC data for two Swedish cities, Borlänge and Uppsala (Johari, Shadram & Widén, Sep., 2023). A common application of UBEM is to explain energy retrofit measures for decarbonation of building stock (e.g., (Ferrari & Beccali, 2017), and (Li & Feng. 2025))

#### 1.2. Input data for UBEM

Input data for UBEM encompasses a wide range of detailed information to ensure accurate energy simulations at the building and district levels. Although there has been a wide range of data enhancement methods for building energy simulations (Sharifi et al., 2023), there is still difficulty in acquiring minimum data for UBEM. Minimum UBEM inputs include building characteristics (geometry, materials, insulation), HVAC and lighting specifications, climate and weather data, and occupancy patterns. UBEM integrates data-driven techniques and probabilistic modelling to overcome three main limitations being General Data Protection Regulation (GDPR), input data, and computational power (Wang et al., Jun., 2022).

Piro et al. (Piro, Ballarini and, Corrado) focused on the input data limitations, requirements, and modeling assumptions necessary for UBEM. They highlight how UBEM introduces simplifications, such as aggregated building geometry, which reduces computational costs but also lead to uncertainties in energy performance predictions. De Jaeger et al. (De Jaeger, Lago & Saelens, 2021) showed the importance of advanced sampling methods in input data generation and proposed a probabilistic building characterization approach for archetype buildings to quantify uncertainty in district heat demand arising from modeling

simplifications. Using quantile regression and copula methods, the study focused on the interdependencies between key building parameters like U-values and window-to-wall ratios. The findings underscore the application of advanced data analysis techniques in UBEM to overcome barriers in input data acquisition. Ferrando et al. (Ferrando et al., 2022) developed building archetypes according to occupant behavior schedules in order to provide results close to operational conditions. Bass et al. (Bass et al., 2022) compared UBEM simulation results to measured energy data across a large building stock to highlight biases introduced by using coarse building metadata (archetypes). They conclude that current methods can predict energy demand accurately on the district level. However, on the individual building level, outcomes are subject to significant errors. The authors demonstrated the need for better data resolution and aggregation methods to improve UBEM accuracy in the individual building level. This problem is pronounced strongly when renovation measures are desired as the main outcomes. Renovation measures heavily depend on current individual building conditions.

#### 1.3. Uncertainty analysis and UBEM

Lack of input data and its consequent data enhancement methods for input data and simplifications of models lead to uncertainties in the outcomes (Ferrando, Causone, Hong & Chen, 2020). Several methods exist for quantifying uncertainties in UBEM outcomes, including Monte Carlo simulations (MCS), Bayesian approaches, stochastic modelling, scenario development, and DST ( (Guo, Haris, Sharifi & Saelens, Jan., 2025; Oraiopoulos & Howard, Apr., 2022; Shamsi, Ali, Mangina & O'Donnell, Oct., 2020; eonsook Tian et al., 2018; Yan, Tang & Li, 2024)). Kong et al. (Kong et al., Aug., 2023) conducted a systematic review of UBEM challenges and opportunities, focusing on the methods, tools, and workflows that are currently adopted. The paper identifies significant gaps in input data collection, model calibration, and simulation methods, highlighting the complexity of urban energy systems and the need for more integrated and scalable UBEM approaches. On the other hand, it has been explored how lack of accurate input data can impact the outcomes of UBEM (Geske, Engels, Benz & Voelker, Sep., 2023). However, current models often fail to address uncertainty comprehensively, particularly in output interpretation (Kong et al., Aug., 2023). A conventional method only shows the range of possible outcomes without identifying their likelihood and significance to guide the decision-makers in interpretation.

One of the most common probabilistic approaches in UBEM is MCS [33], where multiple simulations are run using random input values drawn from probability distributions ((Lin et al., 2023; Ohlsson & Olofsson, May, 2021)). These distributions represent uncertainties in parameters such as insulation levels or HVAC efficiency. By running thousands of iterations, Monte Carlo methods generate a distribution of possible outcomes, providing insights into the likelihood of different energy performance scenarios. Prataviera et al. (Prataviera, Vivian, Lombardo & Zarrella, Apr., 2022) evaluated the impact of input uncertainty on UBEM by applying forward uncertainty analysis (UA) and sensitivity analysis (SA) to a case study in Milan. Using MCS, the study focused on input parameters like building geometry, envelope properties, and occupancy behavior, which are typically uncertain in large-scale urban models. Notably, the previously observed 80 % overestimation in peak heating demand is reduced to 25 % when stochastic variation is included, illustrating the importance of probabilistic UBEM approaches. Zhan et al. (Zhan, Sezer, Hassan & Wang, Sep., 2023) conducted a comparative analysis of uncertainty characterization methods in UBEM applied to a case study in Qatar. The authors compared a deterministic approach with two probabilistic approaches using different Probability Distribution Functions (PDFs) to propagate uncertainties of input parameters to outputs.

Wang et al. (in Wang et al., 2025) adopted scenario development method and incorporated measurement data to calibrate their building thermal models to achieve high accuracy of energy simulations. Yan et al. (Yan, Tang & Li, 2024) argue that the availability of data for calibration models is always a barrier. Hence, they proposed scenario development method for quantifying uncertainties. On the other hand, limitation of the number of scenarios provides a limited and coarse uncertainty quantification which makes their approach case specific, such as when considering finite future climate scenarios as exercise in Liu et al. (2023). Wang et al. (i Wang et al., 2025) adopted a computationally expensive method that combines statistical models (MCS) and distributions of inputs to provide a refined distribution of outcomes under multiple scenarios. Their method, however, was applied to one office building to find optimal renovation strategy under uncertainty.

Thrampoulidis et al. (Thrampoulidis, Hug & Orehounig, 2023) explain why there is a need for a method to derive near-optimal building energy retrofit measures. They explain the necessity of bottom-up models to derive actionable outcomes. They address the computational challenges of city-scale retrofit optimization by developing scalable surrogate modeling. The authors demonstrated their surrogate UBEM using a case study district with over 1400 buildings. However, the task of developing surrogate models was not simply replicable and the method remains case specific.

Li et al. (Li, Zamanipour & Keppo, 2024) developed a multi-output machine learning model for building energy prediction across different time scales (daily, monthly, and annual), using Bayesian adaptive spline surfaces and deep neural networks. The study demonstrates that multi-output models can capture energy use correlations at multiple scales, significantly improving accuracy and reducing uncertainties and computational costs compared to single-output models. The authors applied Latin Hypercube Sampling for input parameter variability and tested the models on an office building in Tianjin, China addressing energy prediction accuracy and scale accumulation. Hwang et al. (Hwang, Lim & Lim, 2024) adopted Bayesian methods to enhance the prediction of building energy demand by applying corrections to building geometry data. Their approach focused on improving the quality of geometrical inputs, which in turn led to more accurate energy simulations and calculations. However, their Bayesian framework exhibited limitations in distinguishing between buildings that have similar energy consumption but differ in structural or physical characteristics. This limitation is particularly critical in the context of building retrofit planning, where both energy performance and detailed building features must be considered. Dempster-Shafer Theory (DST) is a subset of Bayesian methods and has gained attention as a tool for epistemic uncertainty quantification in building energy modeling. Unlike Bayesian methods that require precise prior probability distributions (ieter Tian et al., 2018), DST works with belief functions to provide lower and upper probability bounds (Deng & entropy, 2016) (belief and plausibility) for outcomes. This allows integration of ambiguous or sparse information from multiple sources, making DST a promising alternative or complement to Bayesian approaches for modeling uncertainty (Deng & Wang, 2021). Xuanyuan et al. (Xuanyuan, Yao, Knefaty & Laurice, May, 2024) investigate the application of DST for sensitivity analysis in evaluating the impact of occupant behavior on building energy performance. The authors combine this approach with machine learning techniques to accelerate data processing and enhance model accuracy. The findings suggest that this hybrid method improves both the reliability of energy evaluations and the cost-effectiveness of building operations by selecting optimal model parameters through global sensitivity analysis. While the study focuses on occupant behavior, it does not explore the broader application of this method to retrofit measures or investment cost uncertainties.

#### 1.4. Gaps and motivation

Overall, probabilistic modelling enhances UBEM's ability to upscale and cope with lack of quality input data. These diverse methods and tools allow UBEM to tackle complex urban energy systems, providing planners with actionable insights for sustainable urban development. However, existing methods are either specifically designed for their applications, or they provide general methods that rely on extensive computational power to repeat simulations with a wide range of input data to propagate uncertainty of outcomes. Climate change impact, occupant behavior, and energy prices are among parameters that contribute to aleatoric uncertainties that have been mostly studied in existing literature.

A major gap in current UBEM approaches is the systemic treatment for propagating epistemic uncertainties. UBEM relies on simplified assumptions, such as clustering techniques, causing inaccuracies and oversights. However, the outcomes are conventionally presented with deterministic Key Performance Indicators (KPIs). This can be due to limitations of building-related input data or high computational costs of uncertainty analysis. Even when uncertainties are reported, they are typically given as just a range of outcomes, with little indication of uncertainty itself as a KPI.. Uncertainty KPI provides the basis for risk management, which is an essential part of investment planning. If uncertainties are not comprehensible, risks can be overestimated leading to rejection of feasible plans. On the other hand, if risks are not predicted and mitigated, failure of one proposed plan can hinder future urban energy planning efforts. We develop and demonstrate a method that can incorporate uncertainty analysis in the planning so that energy planners can weigh it against costs and carbon emissions.

#### 2. Materials and methods

It was previously discussed that UBEM inevitably deploys datadriven techniques to simulate the energy performance of building stock while respecting limitations in GDPR, input data, and computation power. Data-driven techniques for UBEM rely on adoption of the most representative buildings, named archetypes or building clusters, in the district to report the results with minimum error in a deterministic approach. Archetypes are the most probable scenarios of all possible scenarios for a group of buildings of which the precise and granular input data are not available. While uncertainty propagation in this study attempts at reporting a probability distribution of outcomes, enabling a decision-maker to screen optimistic and pessimistic scenarios for an evidence-based decision-making. Current uncertainty propagation in UBEM is typically presented only through the outcomes of different input sets, rather than being explicitly quantified and used as a KPI in decision-making. Besides, generating probability distribution has been practiced using MCS which is computationally expensive and inhibitive on the urban scale.

In this study, we address these gaps by developing a framework that integrates uncertainty quantification using DST, allowing for explicit reporting of uncertainties in investment costs for retrofit scenarios, and operational carbon emissions from households in the district as two chosen design parameters for upgrading energy performance of the case study district. We first apply exploratory data analysis and then employ a clustering approach to group buildings by archetypes. Uncertainty measures and energy related outcomes are derived in next steps. We run building energy simulations to explore the impact of retrofit strategies under different obligatory  $\rm CO_2$  reduction scenarios for the district. The process workflow is illustrated in Fig. 2 and elaborated below.

#### 2.1. Input data analysis

The methodology for this study begins with the collection and processing of input data required for UBEM. The input data generally consists of building geometries, materials, HVAC system specifications, historical energy consumption, and local environmental factors such as weather conditions and solar radiation. Buildings are classified into multivariate clusters based on key parameters such as construction type, physical and geometrical parameters, and heating systems (Li, Zamanipour & Keppo, 2024).

In this study building physical attributes for the case study district

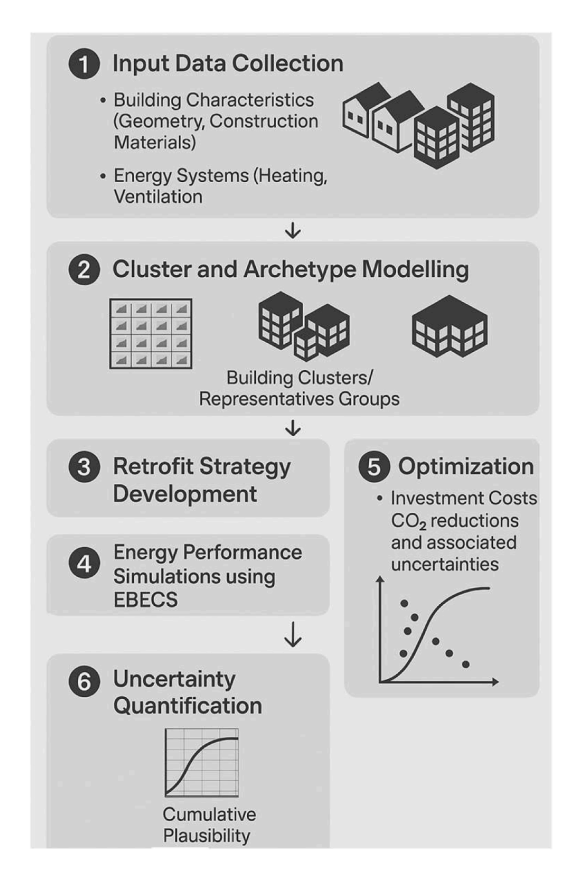


**Fig. 2.** Process workflow deployed using the devised uncertainty quantification methodology.

were provided by the Flemish Institute for Technological Research (VITO) using anonymized Energy Performance Certificate (EPC) data from the Flemish Energy and Climate Agency (VEKA). The data includes distributions of construction year, conductivity of windows, externals walls, roofs, and floors according to the EPC database. Moreover, geometrical attributes such as building floor area, window to wall ratio (WWR), building heights, and building volumes were provided by the VITO dataset aggregated from different sources. An excerpt of the distribution of input data is visualized in the results section within exploratory data analysis and clustering outcomes.

#### 2.2. Building archetypes

In this study, building physical parameters that are involved in uncertainty analysis are specific thermal conductivity of external walls, windows, roof, floor that are required for the energy simulation engine. Geometrical parameters are WWR, total conditioned floor area, and height. The heating system in UBEM is modeled using efficiency of the production unit and fuel type being diesel, natural gas, electricity. Note that we did not include heating system efficiency and type in the uncertainty analysis. Heating systems of the given cases are given as deterministic input parameters. Efficiency of emission system is directly applied to heating system for simplification of data analysis. These eight parameters were chosen for the analysis considering available input data and the importance of parameters in the UBEM outcomes (De Jaeger, Reynders, Callebaut & Saelens, 2020; Ghiassi & Mahdavi, 2017; Menberg, Heo & Choudhary, 2016).

Clustering techniques are common tools to be adopted for deriving representative archetypes where each cluster explains an archetype (De Jaeger, Reynders, Callebaut & Saelens, 2020), (Prina et al., 2024). We use k-means clustering technique which is computationally fast and outperforms other techniques in this application according to the

previous studies such as in (Aggarwal); Goy, Coors and Finn (2021); Dahlström, Johari, Broström and Widén (2024). Results of k-means are also impacted by the scale of the input data and hence the data must be standardized at the first step. The k-means technique uses Euclidean distance (Dahlström, Johari, Broström & Widén, Jan., 2024), (Aggarwal) between data points and center of clusters and aims to find the minimum sum of all distances according to Eq. (1).

$$Dist = \min_{c \in C} \sum_{i=1}^{k} \sum_{\mathbf{x} \in \mathbf{X}} (\mathbf{x} - C_i)^2$$
 (1)

Where Dist is the performance parameter related to Euclidean distance in a multi-dimension domain and C is the center of clusters and the optimization variable. x represents a data point within the set X, which is the set of all possible datapoints, and k is the number of clusters. Defining the number of clusters is not straightforward as explored by Dahlström et al. (Dahlström, Johari, Broström & Widén, 2024). A common approach for determining the optimal number of clusters is named elbow method. It identifies the point where increasing the number of clusters no longer results in a significant decrease in the error metric. In this method, the number of clusters is increased, and the error criteria is reported and monitored iteratively. The iteration stops when the error is not significantly decreasing. However, the error criteria also have been extensively criticized and elaborated (Halkidi, Batistakis & Vazirgiannis, 2001). In this study we used root-mean-square standard deviation (RMSSTD) as proposed by Dahlström et al. (Dahlström, Johari, Broström & Widén, 2024) and calculated using Eq. (2).

RMSSTD = 
$$\sqrt{\frac{1}{n-\nu} \sum_{i=1}^{n} \sum_{j=1}^{k} (x_{ij} - \overline{x_{j}})^{2}}$$
 (2)

Where n is the number of data points, v is the number of variables,  $x_{ij}$  is the value of the i th data point for the j-th variable,  $\overline{x}_j$  is the mean of the j-th variable within cluster.

#### 2.3. Building energy efficiency measures

The building archetypes feed inputs into our energy simulation engine, EnergyVille Building Energy Calculation System (EBECS) (energyville.be/en/product/ebecs-tool), which physics-based monthly steady state energy balance model of the given building. EBECS is a white-box model following Belgian EPC logic for energy demand of residential buildings. It uses a simplified model of heating system accounting for a combined efficiency of production and emission units. EBECS incorporates detailed renovation datasets to simulate energy efficiency measures. These retrofitting measures include improvements in wall and roof and floor insulation, window replacements, HVAC system upgrades, and the integration of renewable energy technologies such as solar photovoltaic panels. Appendix D provides a list of individual building retrofit measures and their specifications. Each archetype's energy performance is simulated both before and after multiple retrofitting to evaluate the potential energy savings, carbon emissions reductions, and associated costs. Retrofit sets are derived from permutation of different individual measures applied to individual building elements, making different combinations of retrofit measures. The choice of energy simulation engine does not form an essential part of this study. The methodology can be replicated with any established building energy and renovation simulation engine.

#### 2.4. Uncertainty propagation

In a deterministic approach, the district is represented by the archetypes derived in the previous section using combined clusters of parameters. However, each cluster takes the parameter values of focal points, while the real values for buildings are distributed. In the developed methodology, we propose using a higher and a lower value limit

for parameter values of each cluster. The lower and higher values form sub-clusters and accordingly form sub-archetypes. The set of all combinations of sub-archetypes for a given archetype defines a probabilistic space characterized by assigned probabilistic. Thus, a deterministic archetype is transformed into a probabilistic representation composed of its sub-archetypes.

In the next step at the district level, various combinations of subarchetypes form a probabilistic space that encompasses all possible configurations representing the district. In other words, each probabilistic event corresponds to a specific set of sub-archetypes that together explain the district. In a deterministic approach, the single set of archetypes with the highest likelihood is used to represent the district. In the proposed method, however, the district is represented by combinations of sub-archetypes, each associated with a given probability. This set of sub-archetypes is then used for energy and retrofit simulations, with the results reported through belief and plausibility distribution functions, as defined by DST explained below.

The DST of evidence, also known as the Theory of Belief Functions or Evidence Theory, is a mathematical framework for reasoning with uncertainty. It generalizes the Bayesian theory of probability and introduces belief and plausibility functions to derive distributions of outcomes without the need for precise input probability distributions (ieter Tian et al., 2018). Moreover, DST provides a means for quantifying epistemic uncertainties by representing what we know about the system through a belief function and weighing it against what we do not know, captured by the plausibility function.

In a deterministic analysis, the district is explained with the original archetypes without a probability distribution. The summation of energy demand for all the archetypes multiplied by the number of buildings in each archetype will show the aggregated energy demand for the district.

In the proposed method, the district is represented with set  $\Theta = \{D_1, ..., D_n\}$  with a probability  $m(D_n)$  for each event Dn.  $D_n$  in our study is formed with a combination of sub-archetypes,  $Dn = \{A_{n+1}, ..., A_{n,m}\}$ , so that each main archetype with identifier I to m must be represented by one and only one of its sub-archetypes in each event Dn. Similar to conventional archetype modeling, each sub-archetype represents a cluster of buildings. The total number of buildings in the district is presented by the summation of buildings in each cluster, and accordingly, related outcomes f(Dn), such as energy demand, carbon emissions, and costs are multiplied by the number of buildings in each sub-archetype and aggregated as shown in Eq. (3).

$$f(Dn) = \sum_{i=1,m} f(An, i) * Ni$$
(3)

Where, m is number of original archetypes and their identifier, whereas n is the identifier of event Dn.  $N_i$  is the number of buildings in sub-archetype i. DST investigates all possible combinations of events in  $\Theta$  in a set named power set  $(2^{\Theta})$ . As such, DST makes sure that any information that is available to support any event from  $\Theta$  will be counted in the analysis (present in the power set) and hence absence of knowledge about the system is reflected. Summation of probabilities of all possible events in the power set  $2^{\Theta}$  equals to 1 as shown in Eq. (4) according to DST.

$$\sum_{D\subset 2^{\Theta}} m(Dn) = 1, \text{ s.t. } m(\varnothing) = 0$$
(4)

To calculate probability of each event  $D_{n}$ , m(Dn), probability of its sub-archetypes must be calculated first. Each sub-archetype has an associated probability mass function named Basic Probability Assignment (BPA) (Fei, Xia, Feng, & Liu, 2019). BPA of sub-archetypes is function of BPA of its parameter's values. Simply put, sub-archetypes with more probable parameter values will themselves be more probable. We propose using PDF to derive probability mass functions for BPA for each parameter according to the available distribution of input data (Xu, Deng, Su, & Mahadevan, 2013). This allows automating and upscaling the process, hence realization of the method in the application

of UBEM. Additionally, our method enables the adoption of low-quality and limited-quantity data as a practical approach to advancing UBEM.

To derive BPAs for all parameters, we fit a kernel density function to each parameter distribution for each archetype. Then, the data range is discretized, and the data are clustered. If only one cluster is used, the BPA will be equal to 1, corresponding to the focal point of the cluster, resulting in a deterministic view of that parameter. We use two clusters for each parameter, providing two focal points representing the upper and lower limits of the range for that parameter. The cumulative probability of the cluster within the parameter is assigned to the focal point of the cluster hence BPA is derived for that parameter value (Fig. 3, left). The procedure is repeated for all parameters involved in the analysis and for each archetype. Choosing the number of clusters for each parameter, as seen in Fig. 3 (right side), gives control over the final number of subarchetypes. Higher number of clusters will exponentially increase the number of sub-archetypes and hence number of simulations while providing a more refined distribution of final outcomes.

BPA mass functions of different parameters with lower and higher values within an archetype are then combined to generate the subarchetypes. Combined BPAs are derived by multiplication of BPAs of individual parameters and then standardized because they are assumed independent events following rules for joint probability. Similarly, BPA of combination of sub-archetypes  $D_n$  is calculated using multiplication of individual BPA of sub-archetypes in each  $D_n$ . Hence, each  $D_n$  will be assigned a BPA named m(Dn) representing probability mass function of Dn. This mass function is also assigned to the outcomes related to that Dn previously shown as f(Dn).

Finally, DST measures named belief and plausibility functions are used to propagate uncertainty. Bel(A) and Pl(A) are calculated using equations Eq. (5) and Eq. (6).

$$Bel(Dn) = \sum_{Dn \subseteq D} m(Dn)$$
 (5)

 $Bel(D_n)$  can be interpreted as a measure for the amount of information in  $D_n$  that intersects with other events in total D.  $Bel(D_n)$  shows how much scenario  $D_n$  that explains total district D is supported by evidence and available input data according to  $A_1$  to  $A_m$  as sub-archetypes.

$$Pl(Dn) = 1 - Bel(\overline{Dn}) \tag{6}$$

 $Pl(D_n)$  represents the absence of information to support  $D_n$  since  $\overline{Dn}$  represents discriminated sets of  $D_n$ . Each  $D_n$  contains required input data for energy simulations and retrofit analysis in addition to BPAs, belief,

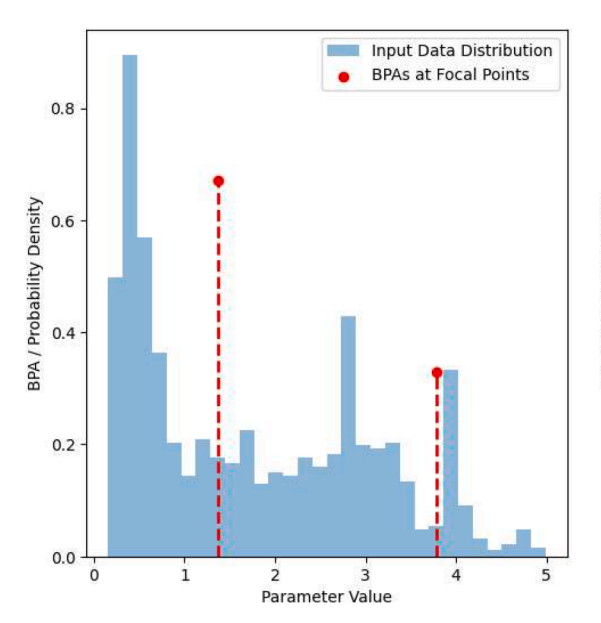
and plausibility functions. Belief and plausibility functions can be reported in cumulative format, named cumulative belief function (CBF) and cumulative plausibility functions (CPF), to provide a decisive measure. CBF means all the evidence that support set  $D_n$  and associated energy demand and costs. Similarly, *CPF* means all the evidence that support  $\overline{Dn}$  and associated calculated outcomes. Uncertainty is understood as the gap between these belief and plausibility of set  $D_n$  (Fig. 4). Algorithm 1 instructs a high-level stepwise flow required for calculation of DST measures for the entire district.

To capture epistemic uncertainties, sub-archetypes were generated by discretizing the parameter ranges of each original archetype. Specifically, for each of the seven key parameters (e.g., wall U-value, window U-value, floor area, etc.), two representative values were selected — a lower bound and an upper bound — based on the distribution of available data. This resulted in  $2^7$ =128 possible combinations per archetype, representing all permutations of lower and upper bounds across the eight parameters. Each combination defines a unique sub-archetype with a specific set of parameter values.

All possible combinations were generated without imposing hard constraints, to fully explore the uncertainty space. However, subarchetypes with physically unlikely combinations naturally receive lower BPAs based on their lower likelihood in the empirical data distributions. This process ensures that the DST framework properly reflects the confidence associated with each sub-archetype while avoiding manual bias.

#### 2.5. Optimal design: collective and individual building retrofit scenarios

To assess the optimal retrofitting strategies, we enforce energy efficiency measures in two steps: collective retrofitting scenarios for the entire district to achieve district level targets in addition to individual building level minimum energy efficiency requirements. The optimal renovation package can be found considering different objective functions.  $\rm CO_2$  emissions, investment costs, and total cost of ownership are among the most common KPIs to include in the objective function. However, this study aims for a simplified objective function to allow for a better interpretation of the outcomes. Moreover, aleatoric uncertainties such as weather conditions, energy prices, and occupant behaviors are not included in the analysis. Thus, we prioritize investment cost over other financial variables such as operational costs and total cost of ownership to avoid facing uncertainties due to energy price fluctuations, taxes, or subsidies, and to isolate the impact of epistemic



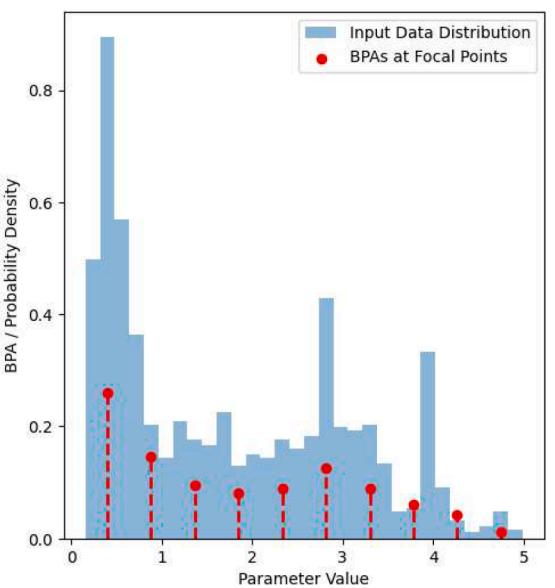


Fig. 3. Comparison between BPAs for two (left) and eight (right) clusters using proposed method. BPA is calculated for focal points using their probability density.

Fig. 4. Uncertainty of set A as a function of Bel(A) and Pl(A) (Deng & Wang, 2021).

#### Algorithm 1

Deriving sub-archetypes and assigned BPAs.

for all archetypes do

for all parameters do

Find lower and higher parameter limits Find BPA for parameters limits using KDE

end for

Combine parameters and form sub-archetypes

Combine BPAs of parameters and derive BPAs of sub-archetypes

end for

Combine sub-archetypes to form Dn

Calculate combined BPAs for Dn

Calculate Bel(D) and Pl(D) for all possible Dn

uncertainty on retrofit strategies. The optimization problem is mathematically formulated as below.

$$\min_{r} o = \sum_{i}^{n} I_{i}^{r} \tag{7}$$

subject to:

$$\sum_{i}^{n} c_i^r < obj. \sum_{i}^{n} c_i^c \tag{8}$$

$$EPC_i^r < 100 (9)$$

 $\forall r \in Rsetandi \in [1:m]$ 

The objective function o in Eq. (7) is summation of the investment costs (I) to be minimized on the district level for renovation packages r as optimization parameter. r is a renovation package from the total renovation options Rset for each building i from all m building archetypes. One optimization constraint is shown in Eq. (8), representing summation of  $C_i^r$  as carbon emissions from building i under renovation package r. This serves the district level carbon reduction objective applied by the scalar parameter obj defining the percentage to which the emissions are required to decrease in comparison to summation of  $C_i^c$  as carbon emission from building i in current situation. Eq. (9) shows another constraint which is EPC requirements for individual building level.

In the individual building level, we find renovation packages that upgrade each building archetype to meet a minimum EPC of 100 kWh/ $\rm m^2$ . Such a minimum can be achieved by a variety of renovation packages. To this aim, we model and simulate all possible combinations for renovation measures for each archetype and then filter the outcomes that upgrade each individual building to an EPC lower than 100 kWh/ $\rm m^2/year$ . In a second step, we enforce a CO $_2$  emission reduction target for the entire district. Among all filtered renovation packages for each archetype, the ones that minimize investment costs and minimize carbon emissions are chosen. The optimization algorithm is designed as below.

At the first step, we find pareto front of renovation packages for each archetype. By that, we decrease the number of options that must be explored by the optimization algorithm. Pareto fronts for each building renovation scenarios will decrease the number of options and help to reach optimal solution in brute force method faster (Sharifi et al., 2022). In the next step, we used an evolutionary algorithm to find the combination of renovation for all the archetypes in the district that can minimize the investment cost and respect carbon reduction in the district level. We developed a brute-force method combined with genetic

algorithms to provide educated guesses in each iteration. DEAP library (Fortin et al., July 2012) from python programing language was used to formulate the optimization problem and solve it efficiently. As evolutionary algorithms do not guarantee finding the optimal solution, the process of finding the solutions for the district was repeated, and optimal solutions were compared to reach a convergence among solutions provided by the algorithm. Algorithm 2 summarizes the steps for the proposed optimization algorithm in high level.

#### 3. Case study: Sint-niklaas

Fig. 5 shows a map of part of Sint-Niklaas city used in the analysis as case study with 1410 residential buildings, where each building is classified into different clusters, denoted by a variety of color codes. These clusters represent archetypes based on building characteristics such as geometry and insulation properties. Note that the cluster colors are only illustrative as we did not need to assign cluster labels to each individual real building for this study. The dataset includes only residential buildings in the Sint-Niklaas district. Non-residential typologies (e.g., commercial, office) are outside the scope of this study and represent an important avenue for future research.

Fig. 6 presents a pair-plot of various building parameters used for archetype modeling in this study. We used window to wall ratio WWR, wall, windows, floor, and roof u-values in addition to building conditioned floor area and height. The data is divided into three building types: detached buildings (green), semi-detached buildings (orange), and terraced buildings (blue). WWR shows a relatively consistent distribution across building types, with most values ranging from 0.1 to 0.3. Detached buildings exhibit a slightly wider distribution, indicating a higher variability in window coverage. Wall U-value, which measures the insulation effectiveness, shows most values clustering between 0.5 to 2.5 W/m<sup>2</sup>K. Detached buildings exhibit a broader range, including some buildings with U-values as high as 3.0 W/m<sup>2</sup>K, indicating poor insulation compared to terraced and semi-detached buildings. Window Uvalue is concentrated between 2.0 and 4.0 W/m2K across all building types, with terraced buildings showing slightly tighter clustering, indicating more uniform window insulation. Floor and roof U-values both show a wide range from 0.5 to 3.0 W/m<sup>2</sup>K, with no distinct patterns separating the building types. However, some detached buildings exhibit very high values for roof U-values, suggesting some buildings may require significant roof insulation improvements. Building Floor Area presents a distinct separation among building types. Detached buildings show the largest variability, ranging from 100 to over 300 m<sup>2</sup>, while semi-detached and terraced buildings generally fall below 200 m<sup>2</sup>. Building Height is another distinguishing factor. Detached and semi-

#### Algorithm 2

Optimization algorithm for optimal de-carbonization scenario.

- 1. Generate a wide range of retrofit plans for each sub-archetype
- $2. \ \ Input sub-archetypes and their retrofit plans into energy simulation engine (e.g., EBECS)$

for all sub-archetypes do

- a. Simulate current situation and all retrofit packages to derive EPC, costs, carbon emissions etc.
- b. Filter packages achieving EPC  $< 100 \text{ kWh/m}^2/\text{year}$  for each sub- archetype
- c. Find Pareto front of packages minimizing investment cost and car- bon emissions end for
- 1. Set district-level Carbon reduction target e.g. 60 percent reductions
- 2. Formulate optimization problem:
  - a. Objective: Minimize district-level investment cost
  - b. Total Carbon emissions less than objectives
- 3. Use evolutionary algorithm (e.g., genetic algorithm with DEAP library)
- 4. Repeat 5 for convergence

Output optimal renovation package for each archetype and district-level summary



Fig. 5. District of Sint-Niklaas, showing different buildings clustered (different colors) into archetypes used for efficient calculations in the UBEM analysis.

detached buildings range mostly between 6 and  $10\ m$ , whereas terraced buildings cluster around  $10\ m$  representing less uncertainty in their geometry.

4. Results

The following section begins by presenting a summary of the clustering analysis and the BPA derivation exercise. This is followed by the optimal renovation solutions, referred to as Pareto fronts, for individual archetypes, and collective retrofit measures for the district under two scenarios:  $80\,\%$  and  $60\,\%$  reductions in operational  $CO_2$  emissions. Next,

the uncertainties across these scenarios are assessed using belief and plausibility functions.

#### 4.1. Clustering and building archetypes

The minimum number of clusters is chosen according to elbow method (Fig. 7). As seen in the graph, the three building types are represented by distinct lines: blue for detached buildings, orange for semi-detached buildings, and green for terraced buildings. For all building types, the RMSSTD metric decreases as the number of clusters increases, meaning that the clusters become more cohesive. However, the

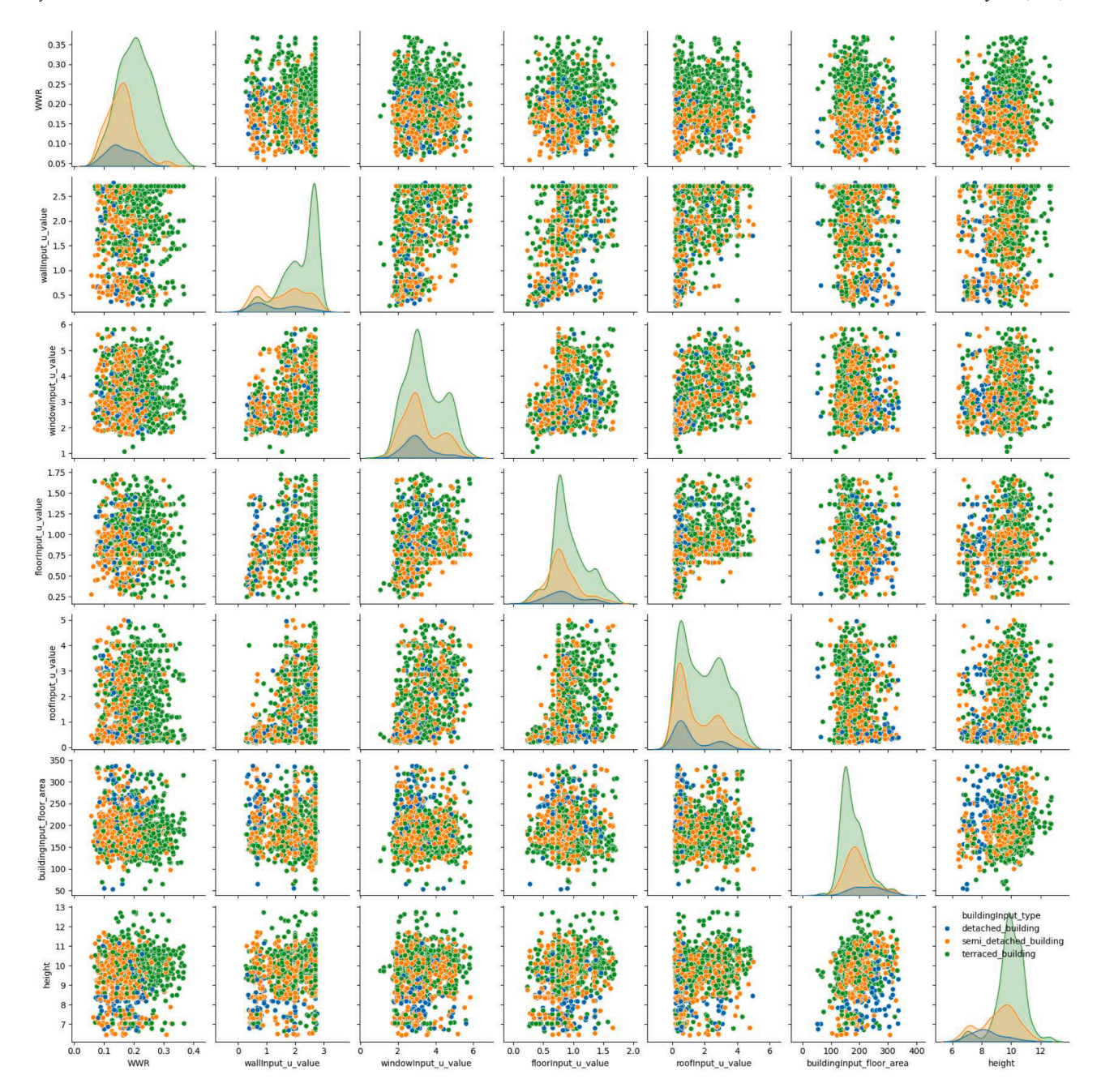


Fig. 6. Pair plot of building parameters (WWR, wall, windows, floor, and roof U-values in addition to building conditioned floor area and height) across detached, semi-detached, and terraced buildings.

improvement in the metric slows down after a certain number of clusters, indicating diminishing returns. The optimal number of clusters appears to be around eight for different building typologies. The clustering results are documented in the table in Appendix A.

Fig. 8 combines box plots with violin plots for various building parameters for one cluster. Red points represent the centroids of cluster derived from the data. The inclusion of centroids in these visualizations provides insight into the original archetypes. For instance, by analyzing the centroids alongside the distributional properties, it is inferred how much real building characteristics can differ from the values taken for the archetypes as focal clusters. To provide intuitive illustration, these variations are reported for d\_6 corresponding to cluster number 6 from detached houses.

Fig. 8 also shows the lower and higher limits for each parameter ofd\_6. d\_6 represents an archetype and combination of these lower and

higher limits for parameter values in  $d_6$  will create sub-archetypes for archetype  $d_6$ . Similarly, each archetype will have multiple sub-archetypes. A complete list of the sub-archetypes with for each single parameter are documented in Appendix B. Afterwards, parameter values and their individual BPAs are combined to provide BPAs for sub-archetypes as documented in Appendix C.

#### 4.2. Optimal solutions

Energy modeling and simulations were conducted for sub-archetypes derived from the upper and lower parameter limits of the original archetypes, as explained above. Renovation packages include improvement in all the physical parameters such as windows and walls, and roof insulation. Heat pump is adopted in all the renovation scenarios if heating system is upgraded as a mandatory renovation measure.

# Elbow Method for Optimal Clusters by Building Type (Hierarchical Clustering) Building Type detached\_building semi\_detached\_building terraced\_building

## Number of Clusters Fig. 7. Comparison between number of clusters and RMSSTD for the elbow method to indicate the optimal number of clusters in three building types.

5

6

7

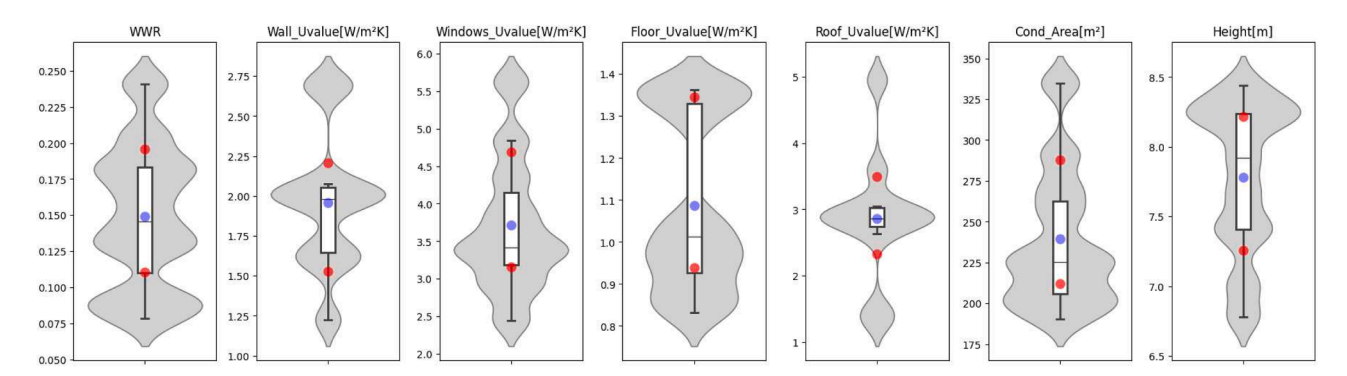


Fig. 8. Comparison between parameter value ranges and their focal points for cluster 6\_d of detached houses. Focal points of parameters used for making sub-archetypes and original archetypes are shown in red and blue respectively.

Installation of PV and its nominal capacity in addition to solar collectors are among renovation packages. Permutation of individual renovation measures in addition to the extent the renovation is applied will create an extensive list of renovation measures. For example, windows can be upgraded to double- and triple-glazing with different quality, accounted with different thermal transmittance coefficient. An excerpt of the outcomes of this intermediate step is shown in this section.

0.65

2

3

4

The scatter plot (Fig. 9) depicts the relationship between investment costs and  $\mathrm{CO}_2$  emissions reduction for two distinct building focal clusters, illustrating trade-offs in retrofitting strategies. Note that the simulations of the original archetypes are not part of the DST analysis and are provided solely to clarify the methodology.

Archetype d\_5 (in red) displays a trend of lower costs and lower emissions, with investment costs ranging from 0  $\[mathscript{\epsilon}$  (current situation shown with black points) to  $1000\ \[mathscript{\epsilon}/m^2$  and  $CO_2$  emissions between 0 and 25 kg/m². Highlighted points differentiate the scenarios by which the EPC will decrease below  $100\ \mbox{kWh/m}^2/\mbox{year}$ . Most points in this archetype are concentrated below  $1000\ \mbox{\epsilon}/m^2$  and  $20\ \mbox{kg/m}^2\ \mbox{CO}_2$ , suggesting cost-effective solutions for moderate emission reductions. In contrast, archetype d\_6 (in blue) spans a wider range of investment costs, from  $500\ \mbox{\epsilon}$  to over  $2000\ \mbox{\epsilon}/m^2$ , with  $CO_2$  emissions ranging from 10 to  $50\ \mbox{kg/m}^2$ . This archetype shows that higher investment levels,

particularly in the 1500–2000  $\rm \epsilon/m^2$  range, tend to correspond with significant CO<sub>2</sub> reductions, as low as 10–15 kg/m². However, some moderate-cost retrofits in this archetype also achieve CO<sub>2</sub> emissions in the range of 20–30 kg/m², offering a balance between cost and emission reduction. The analysis emphasizes the trade-offs involved in retrofitting decisions: archetype d\_6 allows for greater CO<sub>2</sub> reduction but requires higher investments, while archetype d\_5 presents more cost-efficient options with smaller environmental benefits. These findings are crucial for guiding decision-makers in optimizing renovation strategies in the district by balancing financial feasibility and environmental impact.

It was previously explained that each archetype has multiple subarchetypes standing for having a variety of buildings within one archetype. Fig. 10 depicts the relation between carbon emissions and investment costs for renovation packages for all sub-archetypes and their renovation plan within the initial archetype for archetype d\_6. Depending on how the current situation of the building is assumed, the renovation costs and predicted carbon emissions can differ. The Pareto front highlights that there are packages that are sub optimal because they cost more than others and save carbon emissions less than other packages. Pareto front of renovation packages is derived for each subarchetype and used for further developing optimal decarbonization

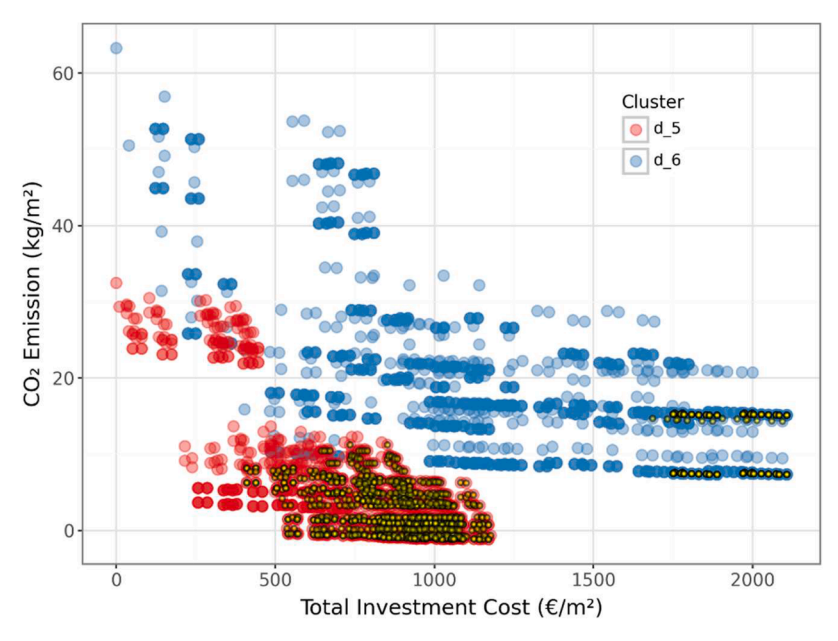


Fig. 9. Comparison of renovation options for archetype d<sub>2</sub>5 and d<sub>2</sub>6 in terms of total investment costs (€/m²) and resulting operational CO<sub>2</sub> emissions (kg/m²).

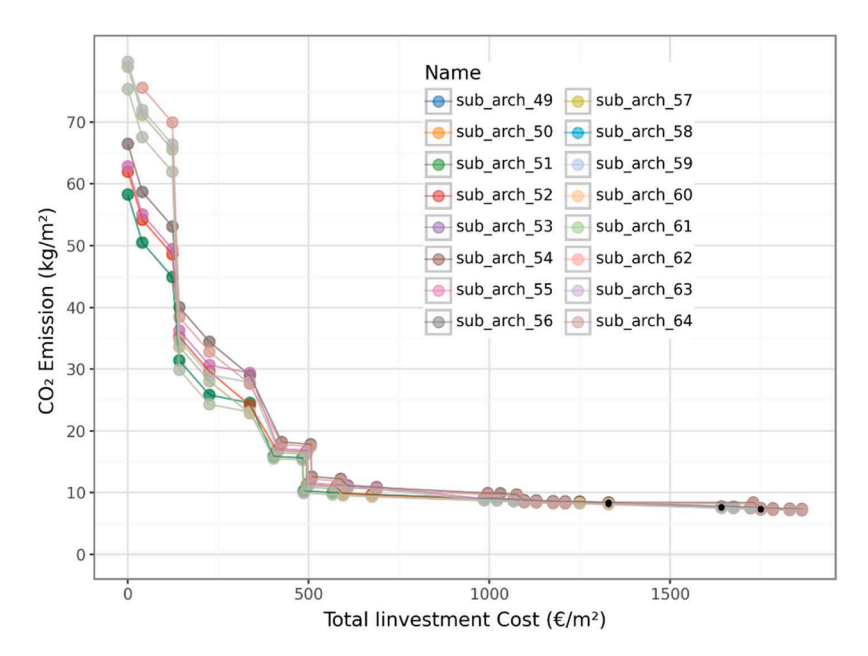


Fig. 10. Pareto front for different sub-archetypes of the original archetype d\_6 from detached houses.

pathway for the district.

In Fig. 10, sub\_arch\_51, shown in dark green, exhibits the lowest baseline emissions at approximately  $55~kg/m^2$ , indicating better initial energy efficiency compared to other sub-archetypes, including the original archetype, sub\_arch\_52. The comparison between different sub-archetypes shows that differences in initial conditions gradually diminish as investment costs increase. The Pareto fronts for each sub-archetype are also depicted in Fig. 10, illustrating the trade-offs between investment costs and carbon emission reductions.

In the next step, optimal design for the renovation package for the entire district was found considering individual and collective objectives. In individual building level, all renovation scenarios that achieved an energy performance of below  $100~\rm kWh/m^2/year$  were first filtered to respect the optimization constraint, representing a legal requirement for building renovations. The collective objective is then respected by the optimization algorithm when proposing renovation packages for each

building. Fig. 11 shows the outcomes of optimization step. Every point represents a renovation package for the district, consisting of renovation scenarios for individual building sub-archetypes in the district. Total investment costs and total operational  $\rm CO_2$  emissions for each point are reported in the point.

The optimization algorithm iterated 500 times for each objective. This was devised because the algorithm is metaheuristic and cannot guarantee finding the global optimal solution. The package with minimum investment cost is chosen as the result of the optimal renovation package for the district for the given objective to continue with the uncertainty propagation.

#### 4.3. Uncertainty analysis

Fig. 12 compares cumulative belief function (CBF) and cumulative plausibility function (CPF) of summation of investment costs for

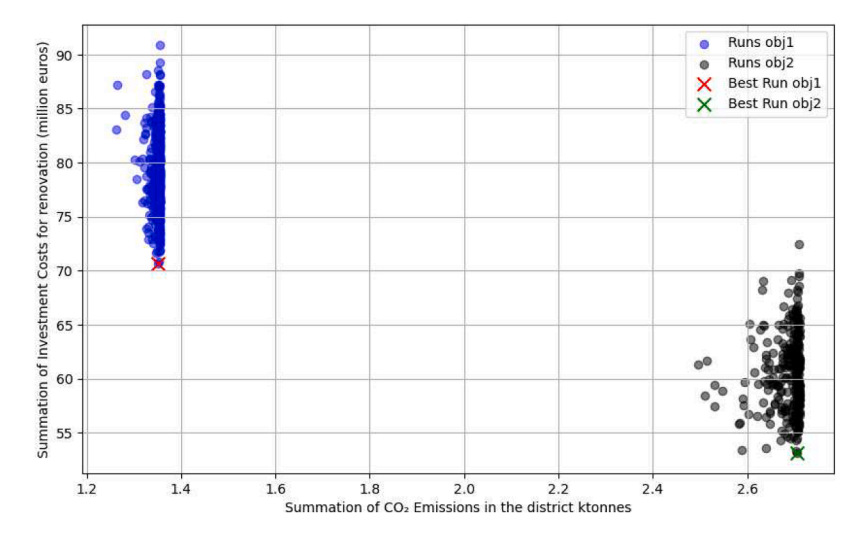


Fig. 11. Trade-off between total investment costs and operational  $CO_2$  emissions in the district under the two scenarios with different carbon emissions reduction objectives obj1 (80 %) and obj2 (60 %). Each dot represents optimal collection of renovation measures for individual building archetypes in the district to achieve obj1 or obj2.

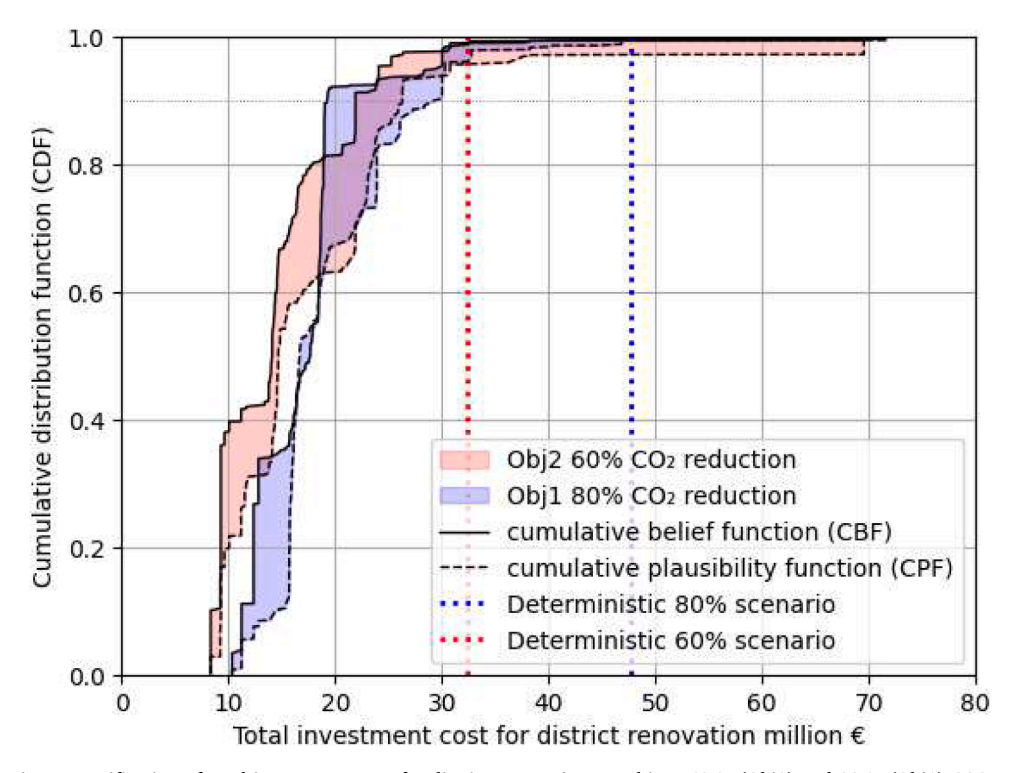


Fig. 12. Uncertainty quantification of total investment costs for district renovation to achieve 60 % (Obj2) and 80 % (Obj1) CO2 reduction targets.

building archetypes renovation under the two intended carbon reduction scenarios, being 80 % (Obj1) and 60 % (obj2)  $\rm CO_2$  operational reductions in the district level. The absolute values of CBF and CPF associated with the investment costs show the level certainty of the costs. Moreover, distance between CBF and CPF reveal how much the investment cost can be deviated for a given certainty level (between 0 and 1).

Fig. 12 demonstrates that achieving the  $80 \% \, \text{CO}_2$  reduction requires higher investments in high uncertainty areas (below 0.6) in comparison to 60 % reduction. For high certainties region the cost difference of the two scenarios is marginal, but there's a risk of steep cost escalation for Obj2 (60 %) above 0.9 CDF. Also, a wider plausibility-belief gap is detected in this region. The graph also proves that the deterministic prediction of costs for both scenarios are supported with plausibility and

belief functions. It is observed that the deterministic prediction of costs is relatively close to high certainty calculations, especially in lower objective.

Fig. 13 depicts the comparison between CBF and CPF for the two optimal renovation scenarios in addition to the current situation in terms of carbon emissions. The figure illustrates the dramatic differences between deterministic and non- deterministic predictions of the current situation carbon emissions. It also shows how carbon reduction can be significantly different in the two scenarios. However, it is observed that the uncertainties, plausibility-belief gaps, are overall higher than the investment costs.

The graph shows that the deterministic prediction for obj1 aligns with a very low CPF, indicating low plausibility for the deterministic value. In contrast, although obj2 is associated with higher carbon

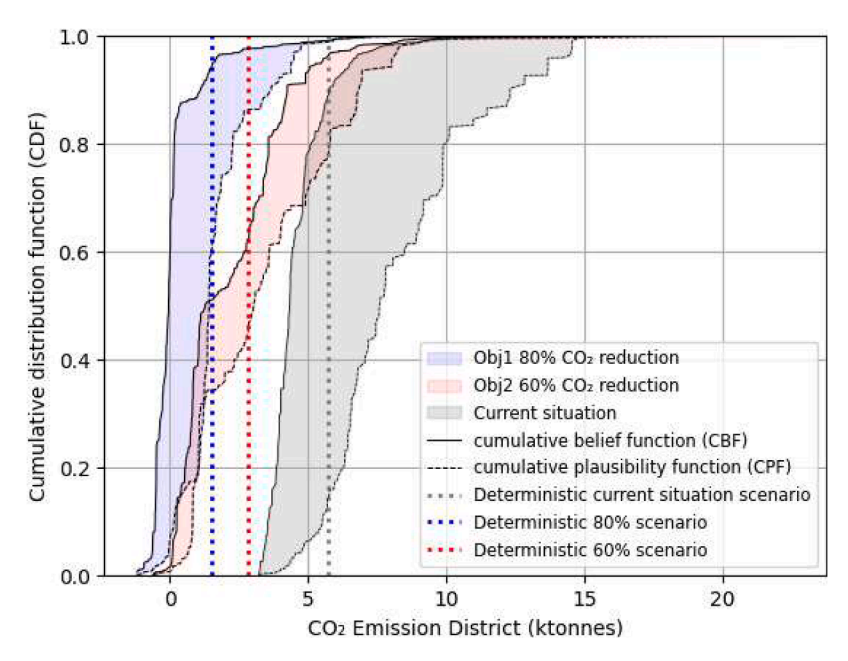


Fig. 13. Cumulative distribution of CBF and CPF of district CO<sub>2</sub> emissions under different scenarios named current conditions, 80 % CO<sub>2</sub> reduction (Obj1), 60 % CO<sub>2</sub> reduction (Obj2), in comparison to deterministic prediction of emissions.

emissions, its deterministic prediction is highly plausible. A significant uncertainty in predicting carbon emissions for the current situation is also observed. Overall, for the current situation the belief-plausibility gap is substantial, particularly for the deterministic value. This difference between the current situation and future scenarios can be explained by the fact that future scenarios like 80 % and 60 % scenarios are constrained by predefined renovation plans, leading to more limited set of options with predictable carbon emissions. Moreover, the 80 % scenario appears to offer a more robust solution for managing uncertainties in the calculation of carbon emissions compared to the current situation. The stark differences in carbon emissions in the 60 % and 80 % scenarios suggest that future building energy policies must adopt a multi-tiered

approach to carbon reduction. The collective targets can help in finding more robust solutions with similar costs. Uncertainty can be also included in the optimization objective function to be minimized when finding the optimal design of the district. The latter will result in a robust optimization problem and requires non-trivial mathematical development to solve the problem.

The belief and plausibility curves for the 80% scenario exhibit a narrower gap compared to the 60% scenario, indicating reduced epistemic uncertainty in both investment costs and carbon emissions. This implies that the 80% scenario is supported by a more consistent set of sub-archetype outcomes, making it more robust despite higher costs

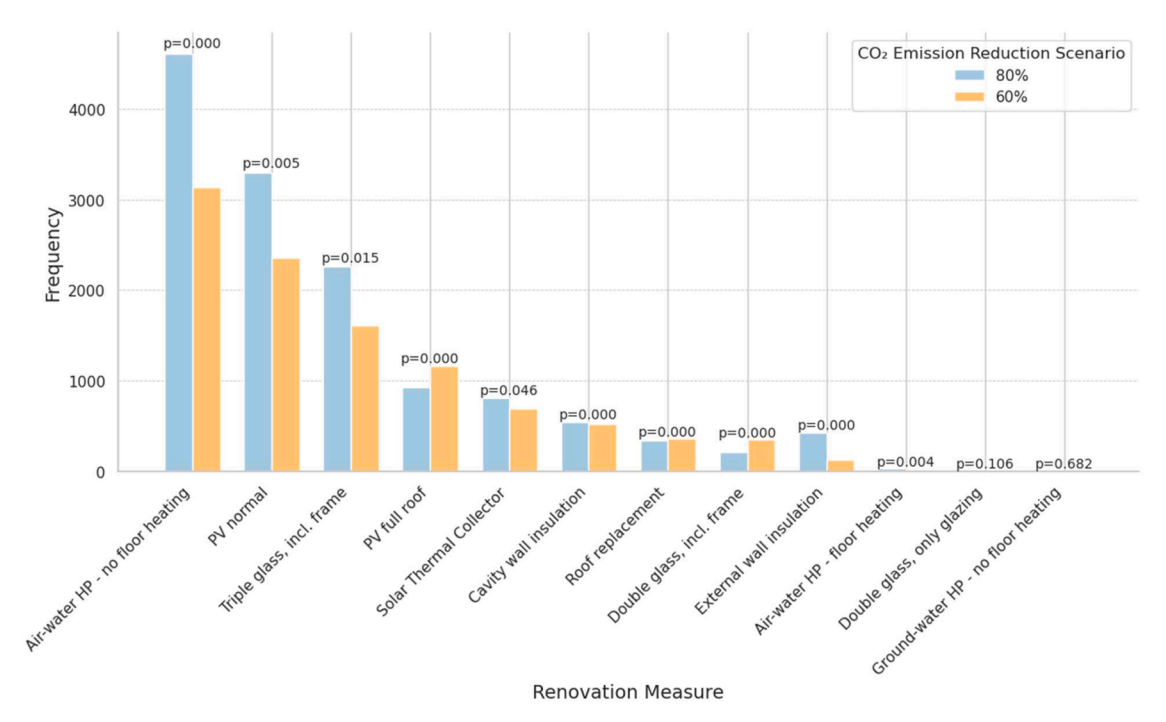


Fig. 14. Comparison of the frequencies of renovation measures selected under the 80 % and 60 % carbon emission reduction scenarios.

#### 4.4. Sensitivity of renovation measures to decarbonization scenarios

It was previously observed in Fig. 11 that the optimization algorithm provides a variety of optimal solutions for building renovations at district level. The optimization outcomes for the two scenarios, 80 % and 60 % reductions in carbon emissions, adhere to their specific constraint boundaries, being 80 % and 60 % carbon emissions reductions for the entire district, while offering different combinations of renovation measures for individual buildings. In this section we further investigate the optimal solutions to decode whether there is meaningful difference between renovation measures proposed by the optimization algorithm for the two scenarios. We first extract frequency of different renovation measures in each scenario and then conduct statistical tests to check if the difference is statistically significant.

Fig. 14 provides a side-by-side comparison of the frequencies of different renovation measures that appeared in all optimal solutions under two distinct scenarios: the 80 % scenario and the 60 % scenario. The p-values annotated above each measure result from a Chi-squared statistical test assessing whether the frequency difference between the two scenarios is statistically significant.

The comparison of renovation measure frequencies between the 80 % and 60 % scenarios reveals clear patterns in technology adoption. Airwater HP without floor heating and normal PV installation emerge as the most frequently selected measures across both scenarios, with significantly higher adoption in the 80 % scenario. Note that PV installation measure in our simulations is a function of building electricity demand. PV size is calculated according to the maximum demand of the building. Normal PV accounts for covering building demand with 35 % self-consumption as assumption, and "full-roof" measure offer larger PVs and assumes exporting electricity to the grid (Appendix D).

Statistical testing confirms that for the major measures, such as heat pump, PV installation, and higher insulations for windows and walls, differences are statistically significant, with p-values below 0.05. This indicates that stricter carbon reduction targets in our simulations lead to a more homogenous uptake of impactful renovation technologies.

#### 5. Discussion

#### 5.1. Further exploration

In this study, a novel methodology was developed and demonstrated for propagating epistemic uncertainties in estimated investment costs and operational carbon emissions associated with collective building renovation strategies at the district level. Compared to conventional approaches, such as MCS, the proposed DST-based method requires significantly fewer energy simulations to generate probability distributions for belief and plausibility functions. This computational efficiency makes the methodology particularly suitable for UBEM applications at city and district scales. An additional strength of the presented method lies in its ability to incorporate expert opinions and incomplete data, making it feasible to conduct uncertainty analyses even in contexts where detailed and high-quality input data are unavailable. The methodology does not particularly need input data distributions because basic mass functions can be given by experts. Moreover, the approach directly quantifies how data limitations translate into uncertainty in projected outcomes.

While an explicit comparison between MCS and DST for the full case study was not feasible due to computational prohibitions (the case study requiring over 70 million simulations under MCS assumptions), comparative studies for individual buildings reported in the literature (ieter Tian et al., 2018; Xuanyuan, Yao, Knefaty & Laurice, May 2024) confirm that MCS outcomes theoretically and practically fall between the belief and plausibility bounds generated by DST, validating the effectiveness of DST in uncertainty propagation. The trade-off lies in reducing both computational effort and input requirements, with the resulting outcomes expressed as bounds rather than single-point values.

#### 5.2. Limitations of the study

The case study results revealed that stricter decarbonization targets (e.g., 80% reduction scenarios) tended to produce more robust and less uncertain outcomes with similar costs compared to less ambitious targets (e.g., 60% reductions). Nevertheless, the underlying causes for the observed variations in uncertainty levels between scenarios were not explicitly identified. Future research should therefore include a detailed sensitivity analysis to investigate whether uncertainty levels correlate systematically with carbon reduction objectives, and to explore the influence of selected retrofit technologies on uncertainty propagation.

A further avenue for improvement lies in analyzing the trade-offs between the number of archetypes and sub-archetypes and the resulting belief-plausibility gaps. While a higher number of sub-archetypes can reduce uncertainty, it also increases computational effort. Identifying an optimal balance between model granularity and computational feasibility would enable more interactive and iterative energy planning workflows, allowing planners to dynamically adjust models as better data becomes available.

From an economic evaluation perspective, investment cost was selected as the primary financial metric to minimize the influence of aleatoric uncertainties such as fluctuating energy prices, taxes, and subsidies. This choice ensured that the study focused purely on epistemic uncertainty arising from building characteristics and retrofit options. Nonetheless, it is acknowledged that this simplification limits the realism of financial outcomes, which could be addressed in future work by integrating Total Cost of Ownership (TCO) or operational cost dynamics under a more sophisticated uncertainty framework.

#### 5.3. Future work

The DST methodology also presents certain challenges. The interpretation of belief and plausibility measures is not straightforward and may require additional processing to be easily usable in decision-making contexts. Measures such as Deng's entropy (Deng & entropy, 2016; Deng & Wang, 2021) offer a way to summarize uncertainty as a single KPI, but these still lack direct interpretability in relation to physical building attributes. Dedicated research on developing more intuitive KPIs linked to DST outputs could further enhance the applicability of this method for practical urban energy planning.

Several modelling simplifications were necessary to make the study tractable, such as assuming uniform occupant behaviour, constant energy conversion factors, and fixed system efficiencies across the building stock. Although these assumptions limit the absolute accuracy of investment and carbon emission estimates, the primary objective of the study was to demonstrate a scalable method for uncertainty propagation, rather than to provide definitive quantitative or qualitative policy recommendations.

Moreover, the DST-based methodology was applied exclusively to residential buildings. It remains an open question how different building typologies, such as commercial, industrial, or office buildings, will impact the sensitivity of belief and plausibility distributions, especially given their more complex and varied HVAC systems, occupancy patterns, and operational schedules. Comparative studies across building types could help to refine DST-based UBEM tools and better target uncertainty mitigation strategies.

#### 6. Conclusions

This study introduces a novel framework for incorporating epistemic uncertainty quantification into Urban Building Energy Modeling (UBEM) through the Dempster-Shafer Theory (DST). By applying this methodology to a case study in Sint-Niklaas, Belgium, we demonstrated the benefits of integrating uncertainty quantification into the planning process for urban energy retrofits. The case study explores the complex interplay between carbon emission reductions, investment costs, and the

technical challenges of retrofitting residential buildings, offering critical insights into the feasibility of achieving collective  ${\rm CO_2}$  emissions reduction targets in the district.

UBEM is increasingly using data-driven methods to simulate the energy performance of building stocks. These methods must account for GDPR rules, limited data availability, and computational constraints. To improve efficiency, UBEM uses representative buildings, called archetypes, that stand in for groups of similar buildings. Archetype modeling can increase computational efficiency with a limited uncertainty of the results. However, it can only provide a deterministic value without indicating the probability of outcomes. While Monte Carlo Simulations (MSCs) can be used to generate probability distributions, they are computationally intensive and prohibitive at an urban scale. They also do not explicitly report uncertainty as KPIs.

This study proposes a framework that integrates uncertainty quantification using Dempster-Shafer Theory (DST). This framework explicitly reports uncertainties with lower computational demand. We derived archetypes of similar buildings and then divided each of them to subarchetypes with associated probabilities, forming a probabilistic space. A methodology was presented to derive probability of sub-archetypes of buildings. A collection of renovation packages was applied to subarchetypes and energy simulations were run to derive carbon emissions and costs before and after retrofits. Optimal renovation packages that respected carbon emissions limitation, being 80 % and 60 % carbon emissions reduction, at district levels were found with an optimization algorithm. Finally, the belief-plausibility gap was reported as an uncertainty measure according to DST.

The comparison of 60% and 80% CO $_2$  reduction scenarios highlights the importance of uncertainty in decision-making. While the 80% scenario demonstrates better environmental outcomes, it requires greater upfront investment, especially in high uncertainty areas. On the other hand, the 60% scenario presents a more financially feasible option with lower initial costs but resulted in higher uncertainties. It was observed that investment costs are prone to more uncertainties in comparison to carbon emissions. This was related to the fact that multiple renovation plans with different investment costs can achieve similar carbon emissions reduction. The clear trade-off between uncertainty and costs of a scenario enables decision-makers to evaluate and mitigate associated risks.

Further research should explore a concise indicator for reporting uncertainty as a KPI. Moreover, conducting a sensitivity analysis on intermediate parameters, such as the number of archetypes and subarchetypes, can enhance the tool's practicality and effectiveness. Finally, future studies should consider integrating dynamic factors such as fluctuating energy prices and occupant behavior to account for both epistemic and aleatoric uncertainties.

### Declaration of generative AI and AI-assisted technologies in the writing process

During the preparation of this work the author(s) used *generative AI tools* to refine the manuscript text. The author(s) wrote the original manuscript and then reviewed and edited parts generated by AI. The author(s) take(s) full responsibility for the content of the published article.

#### CRediT authorship contribution statement

Mohsen Sharifi: Writing – review & editing, Writing – original draft, Visualization, Validation, Software, Project administration, Methodology, Formal analysis, Data curation, Conceptualization. Amin Kouti: Writing – review & editing, Project administration, Investigation. Mohammad Haris Shamsi: Writing – review & editing, Writing – original draft, Project administration, Investigation, Funding acquisition, Data curation. Rui Guo: Writing – review & editing, Project administration. Dirk Saelens: Supervision, Project administration,

Formal analysis.

#### **Declaration of competing interest**

The authors declare that they have no known competing financial interests or personal relationships that could have appeared to influence the work reported in this paper.

#### Acknowledgments

This work was partially supported by PEDvolution project funded by Horizon Europe Framework Programme (HORIZON) under the GA number 101138472, also the Swiss State Secretariat for Education, Research and Innovation (SERI), and Belgian Flux50 ICON "MUPEDD" project funded by VLAIO. Views and opinions expressed are however those of the authors only and do not necessarily reflect those of neither the European Union nor CINEA or other funding institues.

#### Supplementary materials

Supplementary material associated with this article can be found, in the online version, at doi:10.1016/j.scs.2025.106520.

#### Data availability

the data will be partially published as annexes. Part of the data cannot be published.

#### References

https://energyville.be/en/product/ebecs-tool/ accessed on 2nd February 2025.

Aggarwal, CC Data classification: Algorithms and applications (1st ed.). Chapman and Hall/CRC. https://doi.org/10.1201/b17320.

- Ali, U., Shamsi, M. H., Hoare, C., Mangina, E., & O'Donnell, J. (2021, September). Review of urban building energy modeling (UBEM) approaches, methods and tools using qualitative and quantitative analysis. *Energy and Buildings*, 246, Article 111073. https://doi.org/10.1016/J.ENBUILD.2021.111073
- Araújo, G. R., Gomes, R., Ferrão, P., & Gomes, M. G. (2024, December). Optimizing building retrofit through data analytics: A study of multi-objective optimization and surrogate models derived from energy performance certificates. *Energy and Built Environment*, 5(6), 889–899. https://doi.org/10.1016/J.ENBENV.2023.07.002
- Asadi, E., Chenari, B., Gaspar, A. R., & Gameiro da Silva, M. (2023, May). Development of an optimization model for decision-making in building retrofit projects using RETROSIM. Advances in Building Energy Research, 17(3), 324–344. https://doi.org/ 10.1080/17512549.2023.2204872
- Bass, Brett, New, Joshua, Clinton, Nicholas, Adams, Mark, Copeland, Bill, & Amoo, Charles (2022). How close are urban scale building simulations to measured data? Examining bias derived from building metadata in urban building energy modeling. Applied Energy, 327, Article 120049. https://doi.org/10.1016/j.apenergy.2022.120049. ISSN 0306-2619.
- BPIE Buildings Performance Institute Europe. (2021). The renovation wave strategy and action plan: Designed for success or doomed to fail? A review and gap analysis of the Renovation Wave Accessed: Sep. 17, 2024. [Online]. Available: Https://www.bpie.eu/publication/the-renovation-wave-strategy-and-action-plan-designed-for-success-or-doomed-to-fail-a-review-and-gap-analysis-of-the-renovation-wave/.
- Chen, Y, Hong, T, & Piette, MA "City-scale building retrofit analysis: A case study using CityBES", doi: 10.26868/25222708.2017.071.
- Dahlström, L., Johari, F., Broström, T., & Widén, J. (2024, January). "Identification of representative building archetypes: A novel approach using multi-parameter cluster analysis applied to the Swedish residential building stock,". Energy and Buildings, 303, Article 113823, https://doi.org/10.1016/J.ENBUILD.2023.113823
- Dahlström, Lukas, Johari, Fatemeh, Broström, Tor, & Widén, Joakim (2024). Identification of representative building archetypes: A novel approach using multi-parameter cluster analysis applied to the Swedish residential building stock. *Energy and Buildings*, 303, Article 113823. https://doi.org/10.1016/j.enbuild.2023.113823. ISSN 0378-7788.
- De Jaeger, Ina, Lago, Jesus, & Saelens, Dirk (2021). A probabilistic building characterization method for district energy simulations. *Energy and Buildings*, 230, Article 110566. https://doi.org/10.1016/j.enbuild.2020.110566. ISSN 0378-7788.
- Article 110566. https://doi.org/10.1016/j.enbuild.2020.110566. ISSN 0378-7788.

  De Jaeger, Ina, Reynders, Glenn, Callebaut, Chadija, & Saelens, Dirk (2020). A building clustering approach for urban energy simulations. *Energy and Buildings, 208*, Article 109671. https://doi.org/10.1016/j.enbuild.2019.109671. ISSN 0378-7788.
- Deng, Yong, & entropy, Deng (2016). Chaos, Solitons & Fractals, 91, 549–553. https://doi. org/10.1016/j.chaos.2016.07.014. ISSN 0960-0779.
- Deng, Z., Javanroodi, K., Nik, V. M., & Chen, Y. (2023, September). Using urban building energy modeling to quantify the energy performance of residential buildings under

- climate change. Building Simulation, 16(9), 1629–1643. https://doi.org/10.1007/
- Deng, Z., & Wang, J. (2021). Measuring total uncertainty in evidence theory. International Journal of Intelligent Systems, 36, 1721–1745. https://doi.org/10.1002/int.20358
- El Kontar, R., et al. (2020). URBANopt: An open-source software development kit for community and Urban district energy modeling: preprint. *United States* [Online]. Available: <a href="https://www.osti.gov/biblio/1677416">https://www.osti.gov/biblio/1677416</a>.
- EnergyPlusTM. (2017). United States [Online]. Available: Https://www.osti.gov/bibli o/1395882.
- Esfandi, S., Tayebi, S., Byrne, J., Taminiau, J., Giyahchi, G., & Alavi, S. A. (2024). Smart Cities and urban energy planning: An advanced review of promises and challenges. Smart Citie, 7(1), 414–444. https://doi.org/10.3390/SMARTCITIES7010016. vol. 7414–444, Jan. 2024.
- Fei, L., Xia, J., Feng, Y., & Liu, L. (2019). A novel method to determine basic probability assignment in Dempster–Shafer theory and its application in multi-sensor information fusion. *International Journal of Distributed Sensor Networks*, 15(7). https://doi.org/10.1177/1550147719865876
- Ferrando, Martina, Causone, Francesco, Hong, Tianzhen, & Chen, Yixing (2020). Urban building energy modeling (UBEM) tools: A state-of-the-art review of bottom-up physics-based approaches. Sustainable Cities and Society, 62, Article 102408. https://doi.org/10.1016/j.scs.2020.102408. ISSN 2210-6707.
- Ferrando, Martina, Ferroni, Sibilla, Pelle, Martina, Tatti, Anita, Erba, Silvia, Shi, Xing, & Causone, Francesco (2022). UBEM's archetypes improvement via data-driven occupant-related schedules randomly distributed and their impact assessment. Sustainable Cities and Society, 87, Article 104164. https://doi.org/10.1016/j.scs.2022.104164. ISSN 2210-6707.
- Ferrari, Simone, & Beccali, Marco (2017). Energy-environmental and cost assessment of a set of strategies for retrofitting a public building toward nearly zero-energy building target. Sustainable Cities and Society, 32, 226–234. https://doi.org/10.1016/j. scs.2017.03.010. ISSN 2210-6707.
- Fortin, Félix-Antoine, De Rainville, François-Michel, Gardner, Marc-André, Parizeau, Marc, & Gagné, Christian (2012, July). DEAP: evolutionary algorithms made easy. Journal of Machine Learning Research, 13, 2171–2175.
- Geske, M., Engels, M., Benz, A., & Voelker, C. (2023, September). Impact of different input data on urban building energy modeling for the German building stock. *Building Simulation Conference Proceedings*, 18, 2468–2475. https://doi.org/ 10.26868/25222708.2023.1253
- Ghiassi, Neda, & Mahdavi, Ardeshir (2017). Reductive bottom-up urban energy computing supported by multivariate cluster analysis. *Energy and Buildings*, 144, 372–386. https://doi.org/10.1016/j.enbuild.2017.03.004. ISSN 0378-7788.
- Goy, Solène, Coors, Volker, & Finn, Donal (2021). Grouping techniques for building stock analysis: A comparative case study. *Energy and Buildings*, 236, Article 110754. https://doi.org/10.1016/j.enbuild.2021.110754. VolumeISSN 0378-7788.
- Guo, R., Haris, M., Sharifi, M., & Saelens, D. (2025, January). Exploring uncertainty in district heat demand through a probabilistic building characterization approach. *Applied Energy*, 377, Article 124411. https://doi.org/10.1016/J. APENERGY 2024 124411 PA
- Guo, Tong, Bachmann, Max, Kersten, Mathias, & Kriegel, Martin (2023). A combined workflow to generate citywide building energy demand profiles from low-level datasets. Sustainable Cities and Society, 96, Article 104694. https://doi.org/10.1016/ j.scs.2023.104694. ISSN 2210-6707.
- Halkidi, M., Batistakis, Y., & Vazirgiannis, M. (2001). On clustering validation techniques. *Journal of Intelligent Information Systems*, 17, 107–145. https://doi.org/
- Hwang, Jeongyun, Lim, Hyunwoo, & Lim, Jongyeon (2024). Reducing uncertainty of building shape information in urban building energy modeling using bayesian calibration. Sustainable Cities and Society, 116, Article 105895. https://doi.org/ 10.1016/j.scs.2024.105895. ISSN 2210-6707.
- IEA. (2021). Net zero by 2050 Accessed: Sep. 17, 2024. [Online]. Available: Https://www.iea.org/reports/net-zero-by-2050.
- IEA. (2022). Renovation of near 20% of existing building stock to zero-carbon-ready by 2030 is ambitious but necessary Accessed: Sep. 17, 2024. [Online]. Available: Http s://www.iea.org/reports/renovation-of-near-20-of-existing-building-stock-to-zerocarbon-ready-by-2030-is-ambitious-but-necessary.
- IEA. (2024a). Empowering urban energy transitions. ParisAccessed: Sep. 17, 2024.
  [Online]. Available: Https://www.iea.org/reports/empowering-urban-energy-transitions
- IEA. (2024b). Electricity mid-year update July 2024. Paris Https://www.iea.org/report s/electricity-mid-year-update-july-2024.
- Johari, F., Shadram, F., & Widén, J. (2023, September). Urban building energy modeling from geo-referenced energy performance certificate data: Development, calibration, and validation. Sustainable Cities and Society, 96, Article 104664. https://doi.org/ 10.1016/LSCS.2023.104664
- Kamel, E. (2022, November). A systematic literature review of physics-based urban building energy modeling (UBEM) tools, data sources, and challenges for energy conservation. *Energies 2022, 15*(22), 8649. https://doi.org/10.3390/EN15228649. Pagevol. 158649.
- Kong, D., et al. (2023, August). Urban building energy modeling (UBEM): A systematic review of challenges and opportunities. *Energy Efficiency 2023*, 16(6), 1–42. https://doi.org/10.1007/S12053-023-10147-Z. vol. 16, no. 6.
- Li, Pei-Hao, Zamanipour, Behzad, & Keppo, Ilkka (2024). Revealing technological entanglements in uncertain decarbonisation pathways using bayesian networks. *Energy Policy*, 193, Article 114273. https://doi.org/10.1016/j.enpol.2024.114273. ISSN 0301-4215.

- Li, Yang, & Feng, Haibo (2025). Pathways to urban net zero energy buildings in Canada: A comprehensive GIS-based framework using open data. Sustainable Cities and Society, 122, Article 106263. https://doi.org/10.1016/j.scs.2025.106263. ISSN 2210-6707
- Lin, Ziqi, Hong, Tianzhen, Xu, Xiaodong, Chen, Jiayu, & Wang, Wei (2023). Evaluating energy retrofits of historic buildings in a university campus using an urban building energy model that considers uncertainties. Sustainable Cities and Society, 95, Article 104602. https://doi.org/10.1016/j.scs.2023.104602. ISSN 2210-6707.
- Liu, Sheng, Wang, Yuyang, Liu, Xiao, Yang, Linchuan, Zhang, Yingzi, & He, Jingtang (2023). How does future climatic uncertainty affect multi-objective building energy retrofit decisions? Evidence from residential buildings in subtropical Hong Kong. Sustainable Cities and Society, 92, Article 104482. https://doi.org/10.1016/j.scs.2023.104482. ISSN 2210-6707.
- Menberg, Kathrin, Heo, Yeonsook, & Choudhary, Ruchi (2016). Sensitivity analysis methods for building energy models: Comparing computational costs and extractable information. *Energy and Buildings*, 133, 433–445. https://doi.org/10.1016/j. enbuild.2016.10.005. ISSN 0378-7788.
- Ohlsson, K. E. A., & Olofsson, T. (2021, May). Benchmarking the practice of validation and uncertainty analysis of building energy models. *Renewable and Sustainable Energy Reviews*, 142, Article 110842. https://doi.org/10.1016/J.RSER.2021.110842
- Oraiopoulos, A., & Howard, B. (2022,). On the accuracy of Urban building Energy modelling. *Renewable and Sustainable Energy Reviews*, 158, Article 111976. https://doi.org/10.1016/J.RSER.2021.111976
- Piro, M, Ballarini, I, & Corrado, V "From building energy models (BEM) to urban building energy models (UBEM): input data and modelling approaches", doi: 10.26868 /25222708 2023 1662
- Prataviera, E., Vivian, J., Lombardo, G., & Zarrella, A. (2022,). Evaluation of the impact of input uncertainty on urban building energy simulations using uncertainty and sensitivity analysis. *Applied Energy*, 311, Article 118691. https://doi.org/10.1016/J. APENERGY.2022.118691
- Prina, M. G., Oberegger, U. F., Antonucci, D., Ma, Y., Shamsi, M. H., & Sharifi, M. (2024). Clustering of building stock. In H. Doukas, V. Marinakis, & E. Sarmas (Eds.), Machine learning applications for intelligent energy management. Learning and analytics in intelligent systems: 35. Machine learning applications for intelligent energy management. Learning and analytics in intelligent systems. Cham: Springer. https://doi.org/10.1007/ 978-3-031-47909-0-5.
- Shamsi, M. H., Ali, U., Mangina, E., & O'Donnell, J. (2020, October). A framework for uncertainty quantification in building heat demand simulations using reduced-order grey-box energy models. Applied Energy, 275, Article 115141. https://doi.org/ 10.1016/J.APENERGY.2020.115141
- Sharifi, M., Cupeiro Figueroa, I., Mahmoud, R., Himpe, E., Helsen, L., & Laverge, J. (2022). Early-stage optimal design of hybrid GEOTABS buildings in terms of costs and CO2 emissions. *Energy Conversion and Management*, 257, Article 115392. https://doi.org/10.1016/j.enconman.2022.115392. ISSN 0196-8904.
- Sharifi, M., Kouti, A., Lambie, E., Ma, Y., Boneta, MF&, & Shamsi, M. H. (2023). A comprehensive framework for data-driven building end-use assessment utilizing monitored operational parameters. *Energie*, 16, 7132. https://doi.org/10.3390/cp.14207132
- Thrampoulidis, Emmanouil, Hug, Gabriela, & Orehounig, Kristina (2023).

  Approximating optimal building retrofit solutions for large-scale retrofit analysis.

  Applied Energy, 333, Article 120566. https://doi.org/10.1016/j.

  apenergy.2022.120566. ISSN 0306-2619.
- Tian, Wei, de Wilde, Pieter, Li, Zhanyong, Song, Jitian, & Yin, Baoquan (2018b). Uncertainty and sensitivity analysis of energy assessment for office buildings based on Dempster-Shafer theory. Energy Conversion and Management, 174, 705–718. https://doi.org/10.1016/j.enconman.2018.08.086. ISSN 0196-8904.
- Wei Tian, Yeonsook Heo, Pieter de Wilde, Zhanyong Li, Da Yan, Cheol Soo Park, Xiaohang Feng, Godfried Augenbroe, A review of uncertainty analysis in building energy assessment, Renewable and Sustainable Energy Reviews, Volume 93, (2018)., Pages 285–301, ISSN 1364-0321, https://doi.org/10.1016/j.rser.2018.05.029.
- Wang, C., Ferrando, M., Causone, F., Jin, X., Zhou, X., & Shi, X. (Jun. 2022). Data acquisition for urban building energy modeling: A review. *Building and environment*, 217, Article 109056. https://doi.org/10.1016/J.BUILDENV.2022.109056
- Wang, Chao, Wang, Xin, Causone, Francesco, Yang, Yue, Gao, Naiping, Ye, Yu, Li, Peixian, & Shi, Xing (2025a). Addressing uncertainty to achieve stability in urban building energy modeling: A comparative study of four possible approaches. *Building and Environment*, 267, Part B, Article 112197. https://doi.org/10.1016/j.buildenv.2024.112197. ISSN 0360-1323.
- Wang, Wenyuan, Zhu, Li, Zhang, Jiqiang, Zhu, Xingzhe, Yan, Zhexing, & Cao, Mengying (2025b). Evaluation of energy retrofits for existing office buildings through uncertainty and sensitivity analyses: A case study of Tianjin, China. Energy and Buildings, 331, Article 115363. https://doi.org/10.1016/j.enbuild.2025.115363. ISSN 0378-7788.
- Wong, C. H. H., Cai, M., Ren, C., Huang, Y., Liao, C., & Yin, S. (2021, November). Modelling building energy use at urban scale: A review on their account for the urban environment. *Building and Environment*, 205, Article 108235. https://doi.org/ 10.1016/J.BUII.DENV.2021.108235
- Xu, Peida, Deng, Yong, Su, Xiaoyan, & Mahadevan, Sankaran (2013). A new method to determine basic probability assignment from training data. *Knowledge-Based Systems*, 46, 69–80. https://doi.org/10.1016/j.knosys.2013.03.005. ISSN 0950-7051.
- Xuanyuan, P., Yao, J., Knefaty, A. D., & Laurice, S. E. (2024, May). A sensitivity analysis method combining dempster-shafer theory and machine learning for energy-saving

evaluation of building occupant behavior. Journal of Green Building, 19(2), 91-110.

https://doi.org/10.3992/jgb.19.2.91 Yan, Enran, Tang, Changlong, & Li, Yajun (2024). A new workflow for load forecasting in planning areas: Considering uncertainties in building scenarios. Sustainable Cities and Society, 108, Article 105472. https://doi.org/10.1016/j.scs.2024.105472. ISSN 2210-6707. Zhan, D., Sezer, N., Hassan, I. G., & Wang, L. (2023, September). Comparative analysis of uncertainty characterization methods in urban building energy models in hot-arid regions. Building Simulation Conference Proceedings, 18, 2970–2976. https://doi.org/ 10.26868/25222708.2023.1725